Highlights

1. New framework to quantify the heating/cooling effect of urban morphology;
2. Tree height contributes mostly to LST, but varied over cities and seasons;
3. BCR, BH and SDR are the dominant building factors to variations of LST;
4. Human activities significantly affect the heating/cooling effect of buildings;

A new framework quantifying the effect of morphological features on urban temperatures

Fengxiang Guo [1,*], Uwe Schlink [1], Wanben Wu [2], Die Hu [3], and Jiayue Sun [4]

[1] Department of Urban and Environmental Sociology, UFZ – Helmholtz Centre for Environmental Research, Leipzig 04318, Germany; fengxiang.guo@ufz.de; uwe.schlink@ufz.de;

[2] Ministry of Education Key Laboratory for Biodiversity Science and Ecological Engineering, National Observations and Research Station for Wetland Ecosystems of the Yangtze Estuary, and Shanghai Institute of EcoChongming (SIEC), Fudan University, Shanghai, China; wbwu19@fudan.edu.cn

[3] Sino-French Institute for Earth System Science, College of Urban and Environmental Sciences, Peking University, Beijing, China; hudie@radi.ac.cn

[4] Chang Guang Satellite Technology Co., Ltd., Changchun 130000, China; sjy17@mails.jlu.edu.cn

*Corresponding author

Abstract

Urban morphology varies within and among cities. Previous literature well discussed how 2D/3D morphology affects land surface temperature (LST) from physical form, scale and time. However, they focused on ranking the contributions. How quantifying the heating/cooling efficiency and conducting multi-cities comparisons is challenging. This study proposed a new framework to process this issue by integrating cities, scales, and seasons. Among 24 cities close to China's Eastern Seaboard, building coverage ratio (BCR), building height (BH), surface developed ratio (SDR), and tree height (TH) were dominant contributors to LST over seasons. Among them, TH had the highest cooling efficiency, although it varied from cities. For every 1m increase, LST decreased about 0.3℃in northern cities during summer and tiny during winter, while LST decreased about 0.2℃in southern cities during both summer and winter. Economic activities significantly affected the heating/cooling efficiency of dominant building features. High economic levels and population aggregation cause a significant increase in the heating effect of BCR, but a decrease in the cooling effect of BH and SDR, which collectively leads to a warmer environment. According to the results, this study offered several recommendations for better local adaptation strategies of urban transformation, with a focus on heat management.

Keywords: building features, heating/cooling efficiency, land surface temperature, random forest, tree height

1. Introduction

In the century of growing urbanization, with the urban regions expanding by over 20% and urban population increasing by over 30% since 1985, urban morphology constantly transformed and updated in China (Peng et al., 2016; Guo et al., 2022). Building and neighboring environment influence the arrangement of land use and land covers, which can alter the absorption and re-radiation of solar energy, ultimately affecting the urban heat environment (Huang and Wang, 2019; Liu et al., 2021). Moreover, the spatial layouts of buildings are also connected to the level of human activity. A higher building density and volumetric ratio indicate a higher population density and intense land resource development, which in turn causes more energy consumption and artificial heat release (Oke et al., 2017; Song et al., 2020). One well-documented environmental risk is the urban heat island (UHI), which may cause the continuous increase of energy consumption for cooling, environmental pollution and extreme heat events (Zhao et al, 2014; Stewart and Oke, 2012; IPCC, 2022). It has been reported that a 1°C increase of apparent temperature may lead to a 3.12% increase in daily mortality in Mediterranean cities, also a much higher effect in Korea (6.73%-16.3% in six cities) for a similar time period (Baccini et al., 2008). In 2020, the extreme urban heat wave resulted in almost 2500 deaths in England (He et al., 2021).

Land Surface Temperatures (LST) retrieved from remote sensing images offers advantages in terms of coverage, spatial resolution, and cost-effectiveness, making it a more valuable tool for studying the impact of various morphological features on the urban temperature than in-situ observations (Huang and Wang, 2019; Hu et al., 2022). With access of 3D city models, more and more researches are focusing on the influence of buildings on the spatial distribution of urban heat (Berger et al., 2017; Wu et al., 2022). A common approach in these researches is the use of both linear correlation coefficients and nonlinear regression methods. Correlation coefficient is applied

for qualifying the relationship between building characteristics and LST, which may be positive or negative. However, in complex urban environments, this relationship is not straightforward. Random Forest (RF) is often used due to its high interpretability and higher prediction accuracy, as noted by Logan et al. (2020) and Li et al. (2021). RF allows for an assessment of the relative importance of building features for the LST. However, this relative metric does not effectively quantify specific temperature changes and makes comparisons among cities more challenging. Partial dependence plots demonstrate the relationship between the target response and a selected set of input features, while controlling for the values of all other input features (Li et al., 2021; Li and Hu, 2022; Gao et al., 2023). In these cases, partial dependence plots can effectively replace the role of correlation coefficients and provide insight into the temperature changes caused by various morphological features, enabling further comparisons among cities.

Three fundamental elements of urban morphology (physical form, resolution and time) have been well considered when identifying the influence on LST. Physical form refers to the key physical components that structure and shape the city, including land use, street patterns, buildings, and open spaces (Moudon, 1997; Guo et al., 2022). This study focuses on buildings and their open spaces. Buildings within cities vary in terms of function, population density, and urban planning. An increasing body of literature has identified the relationships between urban morphology and LST under different scenarios (Berger et al., 2017; Huang and Wang, 2019; Li and Hu, 2022). The results indicated that both 2D and 3D morphological features (e.g., building coverage, building height, and sky view factor), have a combined effect on LST. However, spatial configuration characteristics are often overlooked. The compactness and irregular arrangement of buildings significantly affect urban ventilation and alter radiation balance patterns and sunshine conditions. Guo et al. (2021) proposed a series of metrics for measuring urban building characteristics from

the perspectives of composition and configuration, and tested their performance in 77 cities in Europe and China (Guo et al., 2022). Besides buildings, the tree height (TH) is another factor that is considered. In general, taller trees can provide more shade and evapotranspiration, which can affect LST (Wu et al., 2022; Yu et al., 2020). However, specific details of the cooling effect remain unknown and further research is needed to fully understand this relationship.

Another aspect is that the physical form varies among cities due to various climate features, economic development, and local architecture culture (Guo et al., 2022; Wu et al., 2022). Changing the experimental setup in traditional studies (depending on specific cases at the city or regional scales), Song et al. (2020) quantified the effects of building density on land surface temperature (K) across 21 cities in China using Landsat 8 imagine. The results suggested a more significant influence of building density on LST in areas with dry climates compared to humid climates. Moreover, Wu et al. (2022) investigated the seasonal relationship between 2D/3D urban morphology and the urban thermal environment in 62 representative large cities across four major climate zones in China. They found significant differences ($p < 0.05$) of seasonal surface regional heat island intensity among climate zones, and the summer LST in cities with humid subtropical climate exceeds approximately 2 °C than the other climate types. Multi-city studies are is important for finding a locally adapted urban temperature mitigation strategy. However, current research does not sufficiently consider the comparison of the influence of urban morphology on LST across multiple cities, particularly the differences of their heating/cooling effects.

The spatial resolution determines the recognizable urban forms, which reflects the plan unit that knead various urban morphological features together for urban planning, and four levels are commonly defined: building/lot, street/block, city, and region (Moudon, 1997; Gauthier and Gilliland, 2006). Grid-based moving window or circle-based sampling methods are widely used

for constructing data pairs of urban morphology and LST (Wu et al., 2019; Li and Hu, 2022). Under different window sizes, associations between building features and LST may vary. Research by Lu et al. (2021), Huang and Wang (2019), and Li and Hu (2022) found that the building coverage ratio was the most significant contributor to variations in LST when the window size was over 120 m, but at a size of 60 m, building height became the most important factor (Li and Hu, 2022). These findings suggest a scale-dependent association between urban morphology and urban heat. At smaller scales, building features, such as building height, can play a significant role by providing shade to the surrounding environment. However, at larger scales, the vertical fluctuation tends to become more relevant, and factors such as building coverage ratio, building spacing, and openness become more important as they affect heat accumulation, ventilation, and the surface energy balance. For that reason, the influence of urban morphology on urban temperatures cannot be fully understood through a single scale analysis and multi-scale studies are required to gain a comprehensive understanding of the relationships and to better guide urban planning (Wu et al., 2019; Lu et al., 2021; Li and Hu, 2022).

Moreover, relationships between morphology and urban temperatures change with season (Lu et al., 2021; Li et al., 2021). The solar radiation varies largely over seasons, causing a periodical variation of LST and various thermal mitigation demands of cities, particularly those in the climate zone with hot summer and cold winter (Ewing and Rong, 2008; Guo et al., 2021). During summer, high temperatures in densely built urban landscapes can exacerbate the effects of urban heat waves and pose a threat to the health of city dwellers. People, particularly the elderly over 65 are more susceptible to heat-related illnesses such as heatstroke, dehydration, and even death, when exposed to high temperatures for a prolonged time (WMO, 2022; Gao et al., 2023). During winter, cold winds remove lots of heat from cities. During this time, protection measures might support the

accumulation of heat and reduce the consumption of energy required to heat the building (Ewing and Rong, 2008). Recent studies on the seasonal influence of urban morphology on LST have a weakness: they mostly rely on LST retrieved from a single remote sensing image, which at best represents only one season. LST is a momentary expression of how the urban landscape affects local surface microclimate; it is easily affected by local weather and atmospheric conditions. Google Earth Engine (GEE) is a platform for geospatial analysis that provides access to over 900 curated datasets and high-performance computing resources for processing them (Gorelick et al., 2017), which offers an efficient tool to generate monthly or annual average LST.

In this study, our goal is to gain a deeper understanding of how urban morphology affects LST in built environments, and a new framework is proposed to quantify the specific temperature changes caused by various urban morphological features through integrating the cities, scales, and seasons. The main objectives of this study are to: 1) identify the dominant urban morphological features that affect LST; 2) extract specific temperature changes through a nonlinear complex regression model; 3) evaluate the heating or cooling efficiency of various morphological features and their potential factors. We expected to uncover the regularities and specificities, and to provide targeted and locally adapted suggestions for a management of the urban thermal conditions to support future urban transformations.

2. Study area and Data

2.1. Study area

China is currently the second-largest economy in the world, with an estimated land area of 9.6 million km^2 and a population of 1.4 billion as of 2019. Since the 1980s, rapid economic development and explosive urban population growth have caused significant variations in urban morphology, including horizontal sprawl, vertical growth, and the transition from traditional to

modern architecture. These changes provide an ideal platform for studying how urban morphology affects the urban heat environment on a large scale. However, the economic development level and spatial distribution of populations are uneven, that the majority of the population and economic development is concentrated to the east, and the south having more frequent economic activities and higher levels of urbanization than the northern region (Gao et al., 2017; Song et al., 2020). We selected 24 cities that are provincial capitals or local economic centers close to China's Eastern Seaboard, with urban populations over 5 million and gross domestic product (GDP) over 50 billion. These cities are distributed across three climate zones: cold region, hot-summer cold-winter region, and hot-summer warm-winter region (Fig. 1).

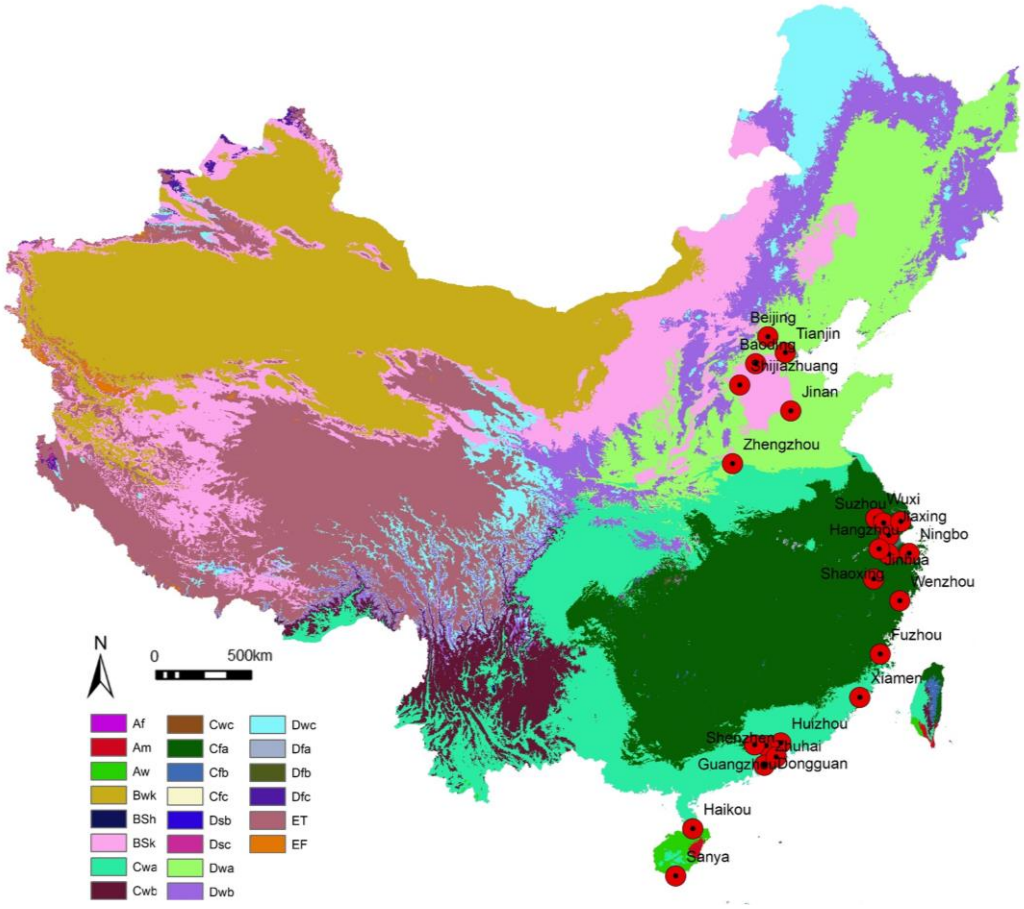

Figure 1. Location of selected cities in China mainland, and spatial distribution of climate zones. Af: tropical-rainforest; Am: tropical-monsoon; Aw: tropical-savannah; Bwk: arid-desert-cold; Bsh:

arid-steppe-hot; Bsk: arid- steppe-cold; Cwa: temperate-dry-winter-hot summer; Cwb: temperate-dry winter-warm summer; Cwc: temperate-dry winter-cold summer; Cfa: temperate-no dry season-hot summer; Cfb: temperate-no dry season-warm summer; Cfc: temperate-no dry season-cold summer; Dsb: cold-dry summer-warm summer; Dsc: cold-dry summer-cold summer; Dwa: cold-dry winter-hot summer; Dwb: cold-dry winter-warm summer; Dwc: cold-dry winter-cold summer; Dfa: cold-no dry season-hot summer; Dfb: cold-no dry season-warm summer; Dfc: cold-no dry season-cold summer; Dfd: cold-no dry season-very cold winter; ET: polar-tundra; EF: polar-frost (Beck et al., 2018).

2.2. Data

From the Landsat 8 satellite data the LST is retrieved at a spatial resolution of 30 m, and using atmosphere correction methods the accuracy is around 1K (Berger et al., 2017; Guo et al., 2021). For selected cities, the map of summer LST (SLST) was generated by averaging the LST from June 1 to September 1 during the period 2018-2020 on the GEE platform. The dates used for generating winter LST (WLST) were from December 1 to March 1 for the same period.

The building height data is gathered from Baidu China Co., Ltd, with an overall accuracy of 86.78% (Guo et al., 2022; Wu et al., 2022). The tree height data, from the Global Forest Cover Change dataset, has a spatial resolution of 30 m and good accuracy, with an RMSE of 6.6 m and a MAE of 4.45 m (Sexton et al., 2013; Wu et al., 2022).

To identify potential factors affecting the heating or cooling efficiency of each morphological feature in each city, economic data, including GDP and urban population (POP), were downloaded from the National Bureau of Statistics of China. Additionally, climate features, including mean air temperature (MAT) and mean humidity (MH), were downloaded from the China Meteorological Administration. Latitude (LAT) and longitude (LON) were also considered as geographic factors.

3. Methods

Data processing comprises five main steps: 1) calculate 23 selected building metrics and tree height for all cities and scales (section 3.1); 2) generate SLST and WLST using Landsat 8 OLI/TIRS remote sensing images on GEE platform; 3) obtain the relative importance of each morphological feature on LST using random forest over cities, scales, and seasons, and then select the dominant building features which belonging to IM1 (see section 3.2.1); 4) extract the specific temperature changes from the partial dependence plots, and further calculate the heating or cooling efficiency of each dominant feature (section 3.2.2); 5) calculate the correlation between the heating or cooling efficiency and their potential factors. Detailed information was shown in Fig. 2.

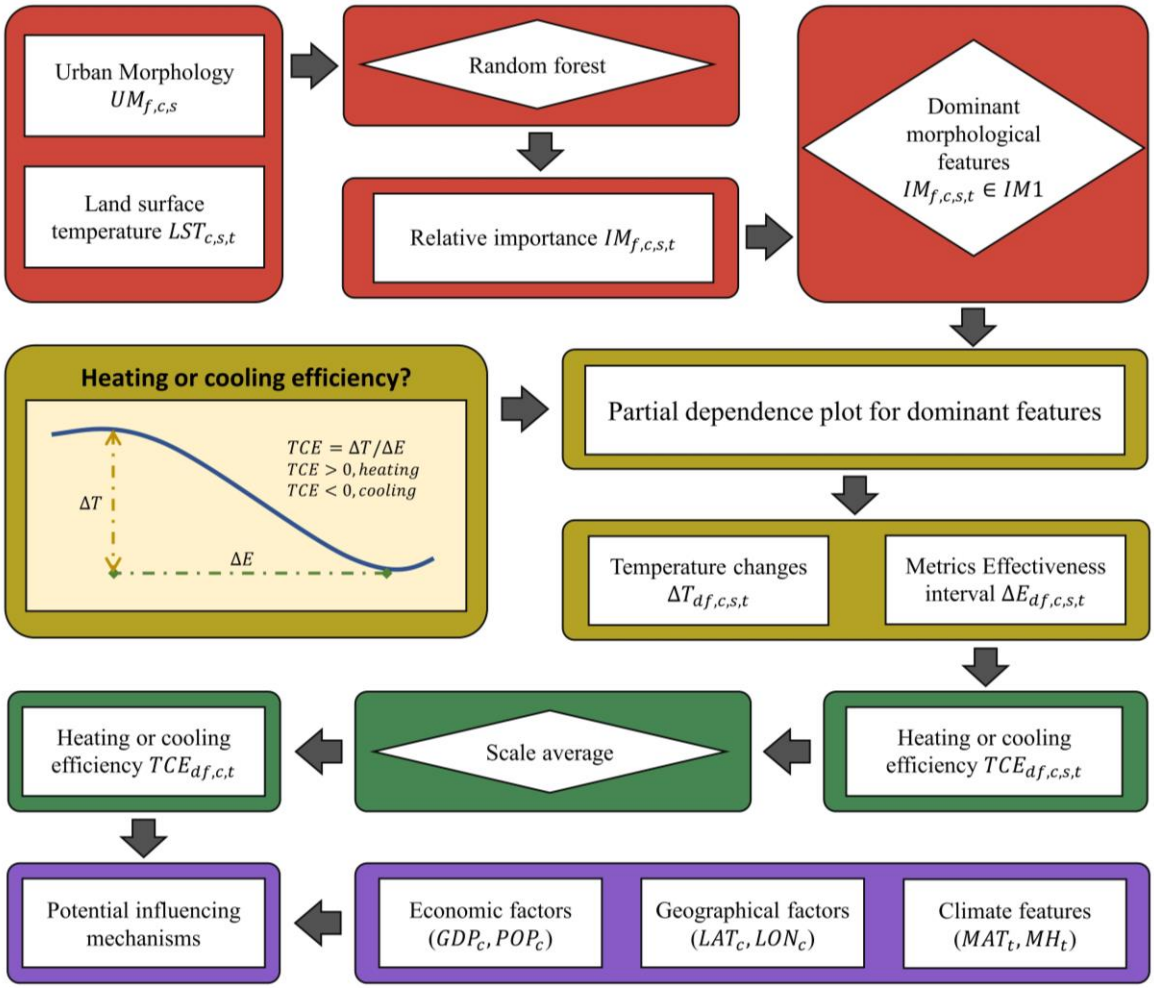

Figure 2. Flow chart of the implementation and analyzing methods.

This study is focused on the built environment, and to avoid the influence of large vegetation and water bodies on the statistical results, only those areas with an impervious surface proportion greater than 0.7 were included to generate data pairs of urban morphology and LST. These areas, referred to as 'windows' in this study, were chosen to ensure that the data reflected the characteristics of urban building layouts. For various scales (ranging from 45 m to 480 m), we recalculated the morphological metrics without spatial aggregation. This approach allowed us to account for the high heterogeneity of urban building layouts and to avoid the influence of the modifiable unit areal problem on the statistical results (Ye and Rogerson, 2022).

3.1. Building metrics

This study utilized the software LPA3D, developed by Guo et al. (2022), to extract building features within cities. LPA3D provides over 45 metrics related to the spatial composition and configuration in 3D space. These metrics are based on patch mosaic and surface gradient models, similar to the definitions used in FRAGSTATS, and are applicable to raster data. Once categorized, boundaries of patches were defined (Kedron et al., 2019). An enclosed building area is taken as a patch, and the class refers to the mixture of different patches with the same or similar height (Kedron et al., 2019; Guo et al., 2021). The built landscapes were divided into 5 classes based on the spatial heterogeneity of building height, namely low buildings (below 10 m), sub-low-rise buildings (10 m – 20 m), middle-rise buildings (20 m – 30 m), sub-high-rise buildings (30 m – 100 m), and high-rise buildings (over 100 m). In the study at hand, 23 building metrics ($= 18 + 5 \times$ PLAND) were chosen, aiming to measure the diversity, complexity, compactness and fragmentation of the built landscape (Table 1).

Table 1. Metrics for measuring urban building features; additionally tree height (TH) was included.

Metrics	Abb.	Type	Measure of the …
Building coverage ratio	BCR	Composition-2D	building coverage degree in a window.
Edge density	ED	Composition-2D	building segmented by the boundary.
Euclidean nearest-neighbor Mean Distance	ENN	Composition-2D	isolation degree of each buildings class, and can be taken as indicator for measuring the road width and building spacing.
Patch density	PD	Composition-2D	evenness and building number of urban building pattern.
Mean building height	BH	Composition-3D	mean height of urban buildings.
Surface area	SA	Composition-3D	surface fluctuation compared with plane area
Mean Volume index	VOL	Composition-3D	mean volume of urban buildings.
Building surface slope	SSL	Composition-3D	integral slope of building surface, which is the sum of surface fluctuation at adjacent building pixels.
Surface developed ratio	SDR	Composition-3D	deviation of building surface to projected plane
Standard deviation of height	SQ	Composition-3D	undulation of the urban buildings surface.
Percentage of patch type	PLAND	Composition-3D	proportion of each buildings class in the urban building pattern, including low-rise (LB), sub-low-rise (SLB), middle-rise (MB), sub-high-rise (SHB) and high-rise buildings (HB).
Landscape shape index	LSI	Configuration	deviation between patch shape and regular circle or square with same area.
Building Shade metrics	CNI	Configuration	effect of buildings forming ventilation paths, defined by the ratio between building height and building spacing (ENN).
Largest patch index	LPI	Configuration	largest space occupation of single building.
Landscape division index	LDI	Configuration	aggregation degree of buildings. LDI = 0 when the landscape consists of single patch
Landscape fractal dimension index	LFI	Configuration	irregularity and complexity of urban buildings landscape shape.
Shannon's diversity index	SHDI	Configuration	diversity of urban buildings landscape.
Cohesion index	COI	Configuration	connectivity and aggregation of the urban building pattern.
Proximity index	PROX	Configuration	proximity, defined by the ratio between building height and square of building spacing (ENN).

3.2. Random forest

The random forest (RF) method is a bagging ensemble learning approach for classification or regression by constructing a multitude of decision trees during training (Belgiu and Drăguț, 2016; Logan et al., 2020). Each decision tree is created with a different, randomly chosen subset of both the training data and the features at every node. For regression, RF can handle high dimensional feature sets well and generate an internal unbiased estimate of generation error, with better prediction accuracy than traditional linear regression analysis (Hutengs and Vohland, 2016; Guo et al., 2022). Compared with deep learning methods, known as 'black box', RF has the advantage of higher readability and interpretation. Additionally, random decision forests correct for decision trees' tendency to overfit their training set by averaging a large number of decorrelated individual trees (Hutengs and Vohland, 2016). In this study, the 24 urban morphological features were taken as independent variables to predict the LST across cities, scales, and seasons. 70% of the data was used as training set, and the remaining data was used to test the regression accuracy, as suggested by the coefficient of determination (R^2).

3.2.1. Evaluation of Relative importance

RF has the ability to rank the relative importance of variables in a regression, which can be applied to judge the sensitivity of morphological features to LST (Hutengs and Vohland, 2016). Variables with high importance are drivers of target response and their values have a significant influence on LST. The relative importance can be calculated using mean decrease accuracy (MDA) methods, which is based on the decrease in accuracy that occurs when a particular variable is not used in a tree for splitting the data (Han et al., 2016; Gao et al., 2023). This method considers the error rate of a tree or forest with and without the variable, and evaluate the contribution of

influencing factors by using the Shapley additive explanations (SHAP) value. The SHAP value of each variable (f) is the average decrease in accuracy over all the trees in the forest.

$$SHAP_f = \sum_{S \in N\{m\}} \frac{|S|!\,(M - |S| - 1)!}{M!} \left[\widehat{LST}(S \cup \{f\}) - \widehat{LST}(S)\right] \quad (1)$$

where N is the set of all features for the training dataset with dimension M, S is the permutation subset of N with dimension $|S|$, $\widehat{LST}(S \cup \{f\}) - \widehat{LST}(S)$ is the difference of predicted value with and without feature f using feature set S. Higher SHAP value means larger importance and contribution to LST. Through comparing SHAP values, we can calculate the relative importance ($IM_{f,c,s,t}$) of each morphological feature (f) over different cities (c), scales (s) and seasons (t). Based on the descending order of relative importance among the variables, five importance levels are defined: IM1 (variables ranked 1 – 5), IM2 (variables ranked 6 – 10), IM3 (variables ranked 11 – 15), IM4 (variables ranked 16 – 20), and IM5 (variables ranked 21 – 24).

3.2.2. Definition of heating or cooling efficiency

The relative importance is an indicator that reflects only the contribution of various features to the variations of LST. It cannot quantify the specific amount of temperature change caused by each feature. The partial dependence plot (PDP) is a useful tool for addressing this issue as it illustrates the dependence between LST and a target feature by marginalizing the impacts from other features (Gao et al., 2023). The PDP can be calculated as follows:

$$\widehat{LST_f}(x_f) = \frac{1}{n}\sum_{i=1}^{n} \widehat{LST}[(x_f, x_c^{(i)})] \quad (2)$$

where x_f is the feature to be plotted against the target ($\widehat{LST}$) to show the relationships; x_c are the other features; n is the number of samples in the dataset. Fig. 3 shows an example of PDP illustrating how building height affects SLST in Beijing using window sizes of 120 m and 300 m,

respectively. In result building height is negatively related to SLST, with a temperature decreases of $\Delta T = 0.3℃$ at the scale 120 m and that of $\Delta T = 0.1℃$ at the scale 300 m.

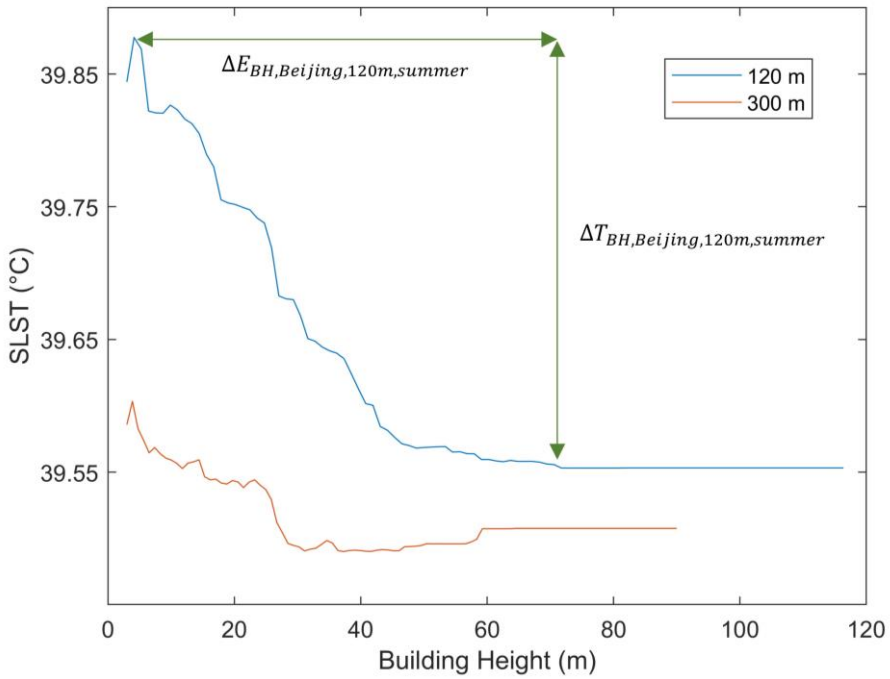

Figure 3. PDP of the relationship between building height (BH) and SLST in Beijing with window sizes of 120 m and 300 m.

In addition, LST tends to stabilize when building height increases to 73 m at the scale 120 m, but LST becomes stable already at 30 m for the 300 m window size. Assessing the effective and monotonous temperature change (ΔT) of LST depending on the morphological feature in its effectiveness range (ΔE), we determine the heating or cooling efficiency as:

$$HCE_{f,c,s,t} = \Delta T_{f,c,s,t} / \Delta E_{f,c,s,t} \quad (3)$$

$HCE > 0$ indicates the heating efficiency that represents a positive association between LST and the morphological feature. Conversely, $HCE < 0$ indicates the cooling efficiency having a negative relationship between the feature and LST. Considering that features with lower

importance are less sensitive to LST, we applied a filter to extract and only chose with a relative importance of IM1 to calculate the $HCE_{f,c,s,t}$. These metrics are taken as dominant features (df).

4. Results

The accuracy of the predicted SLST and WLST remained consistently high across different window sizes, with the lowest R^2 (0.77 and 0.76) observed at a window size of 45 m. As the window size increased, the mean R^2 value tended to increase for both SLST and WLST (Fig. 4), indicating that the selected morphological features exhibited sensitivity to variations in LST during both summer and winter.

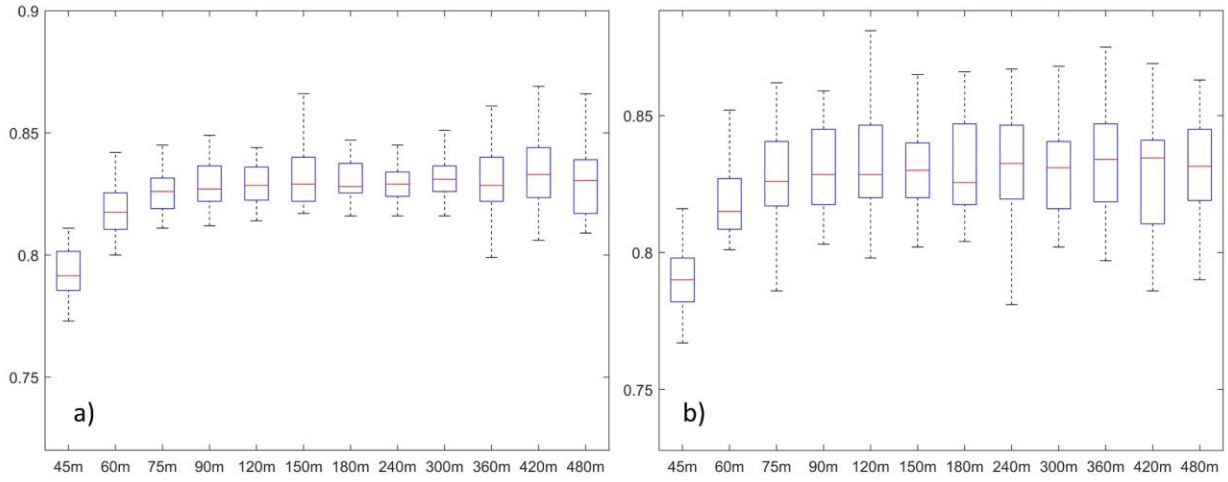

Figure 4. R^2 of predicted LST in terms of window size during summer (a) and winter (b). Each box represents the R^2 for all cities at specific scale, and the red line indicates the median value.

4.1. Dominant morphological features affecting SLST and WLST over cities and scales

Appendix A1 and A2 displayed the relative importance of each morphological feature among scales during summer and winter, respectively. Based on the median value of each box, tree height (TH) had the highest contribution to the variations of LST for most cities, especially during summer, with a relative importance ranking first (Appendix A1). During winter, there was greater fluctuation in relative importance values among cities for each scale, but the median values still

belong to IM1 across scales (Appendix A2). Among building features, building coverage ratio (BCR), building height (BH), and surface developed ratio (SDR) showed higher importance on both SLST and WLST, as suggested by the median values of relative importance. However, the results do not allow for distinguishing their positive or negative association with LST, and are unable to extract specific temperature changes.

4.2. Heating or cooling effect of dominant morphological features

After scale averaging of $\Delta T_{df,s,c,t}$, positive values were observed for BCR across cities and seasons, indicating a significant heating effect of building coverage (Fig. 5). As BCR increased, SLST increased by approximately 0.8 ℃, with a greater increase observed in northern cities such as Beijing, Tianjin, and Jinan than in southern cities such as Xiamen, Shenzhen, and Sanya (Fig. 5). The increases in WLST due to BCR were generally less than 0.4 ℃ across cities, which is much lower than those observed during the summer. BH, SDR and TH were negatively related to both SLST and WLST, which indicates a cooling effect of these urban morphological features. Similar to the relative importance, the cooling effect of TH was much stronger than for the others. The decrease in SLST was greater than that in WLST for each city. During the summer, the greatest cooling effect caused by TH was a decrease of 5.3 ℃ observed in Shanghai, with no significant differences in the cooling degree among cities in the north and south. During winter, there were noticeable regional differences in the cooling degree. In the north, there was no apparent influence of TH on WLST, but in the southern cities, the temperature decreased significantly. BH and SDR had a similar cooling effect during both summer and winter, resulting in an average temperature decrease of around 0.5 ℃ across cities.

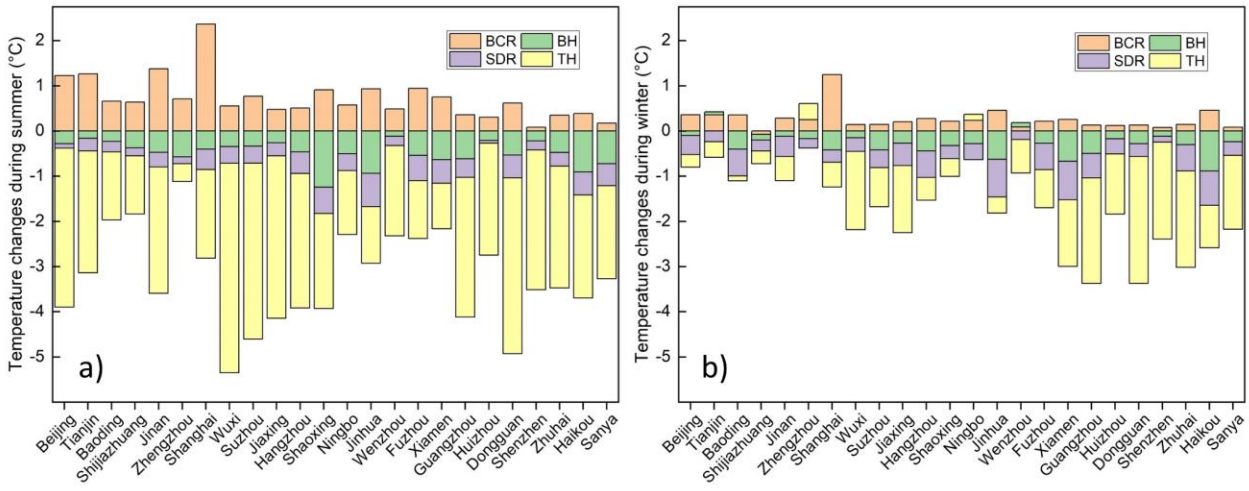

Figure 5. Temperature changes of SLST (a) and WLST (b) caused by the dominant morphological features. Positive (negative) values indicate heating (cooling) effects. The horizontal axis represents the city, ordered from left to right in their geographic location from north to south.

Significant seasonal differences were observed in the heating efficiency of building coverage ratio (BCR) and cooling efficiency of tree height (TH), with stronger effects during summer than winter, while the cooling efficiency of building height (BH) and surface developed ratio (SDR) exhibited an opposite trend (Fig. 6). Specifically, during summer, the heating efficiency of BCR varied across regions, with a higher increase in LST of over 1 ℃ observed in the northern cities compared to around 0.8 ℃ in the southern cities for every unit increase in BCR. This indicates a much more significant influence of BCR in the north. Moreover, the heating efficiency of BCR decreased significantly from summer to winter, with the largest effects observed in Shanghai. Regarding TH, during summer, SLST decreased by over 0.3 ℃ for 1 m increase in TH in the northern cities, but the effects almost disappeared during winter. In contrast, for the southern cities, the cooling efficiency of TH remained relatively stable during both seasons, with LST decreasing by 0.2 ℃ for 1 m increase in TH. Similarly, the cooling efficiency of BH exhibited seasonal differences, with a tendency to increase from summer to winter, but it varied among cities.

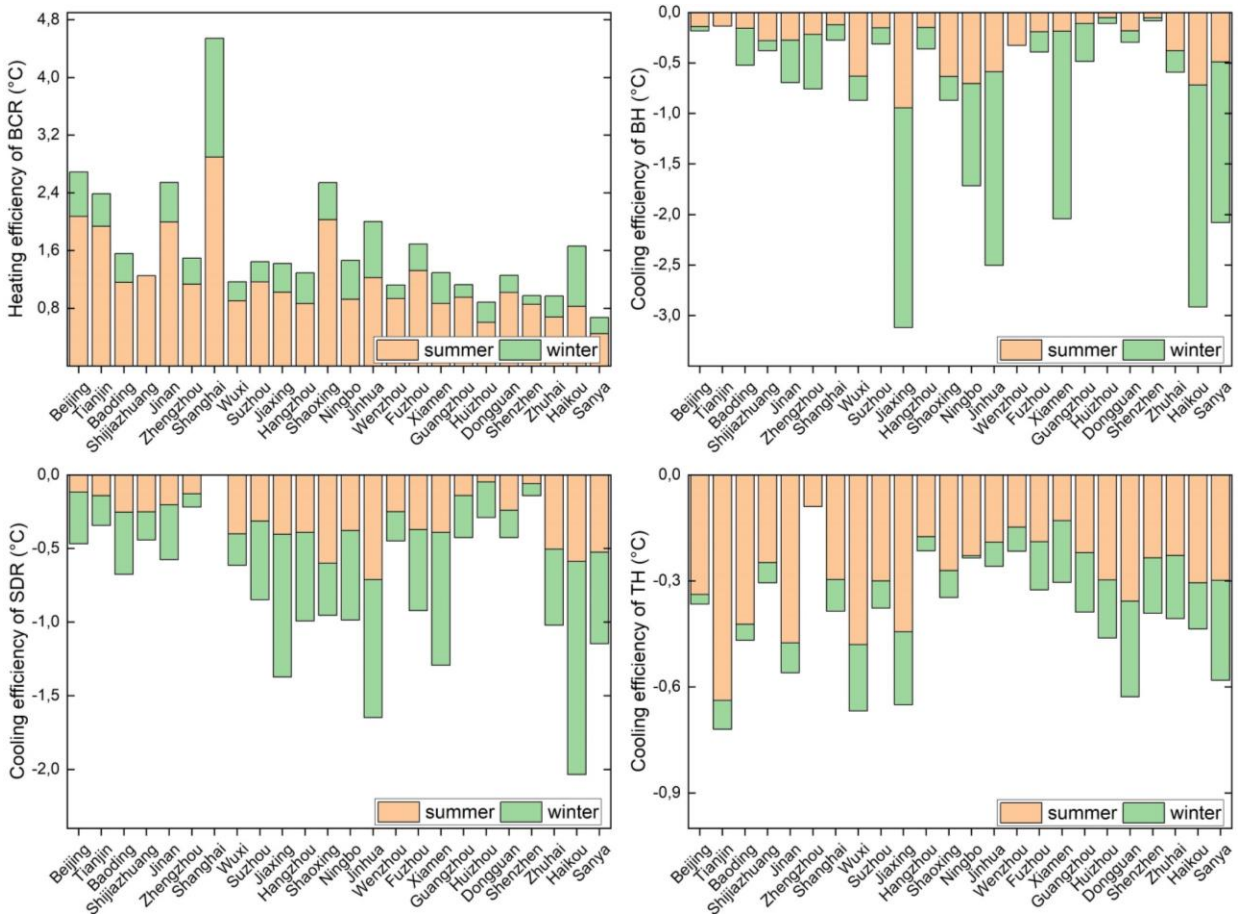

Figure 6. Heating efficiency of building coverage ratio (BCR, top left) and cooling efficiencies of building height (BH), surface developed ratio (SDR), and tree height (TH) in summer and winter.

4.3. Potential factors affecting the efficiency of heating or cooling

The building features influencing LST, including the heating efficiency of BCR as well as the cooling efficiency of BH and SDR, are correlated to economic factors (Table 2). During summer, the Gross Domestic Product (GDP) and urban population (POP) are positively correlated with the heating efficiency of BCR (0.56 and 0.63, respectively), but negatively related to the cooling efficiency of BH (-0.47) and SDR (-0.56). These relationships contribute to a warmer urban environment, especially in larger cities with higher economic levels and greater urban populations. A similar pattern was observed during winter, although with lower correlation coefficients. Furthermore, as expected, the heating efficiency of BCR during summer is negatively related to

mean air temperature (MAT) and mean humidity (MH), with correlation coefficient -0.42 and -0.47, respectively. The cooling efficiency of trees is significantly influenced by latitude (LAT), but the associations are opposite during summer (0.39) and winter (-0.69). This is due to the significant seasonal variations of the cooling efficiency of TH in the northern cities, but relatively stable variations in the southern cities.

Table 2. Correlation coefficients between heating or cooling efficiency and their influencing factors during summer and winter. Red circle means a significant positive correlation, while green circle means a significant negative correlation under the significance level 0.05.

	GDP	POP	LAT	LON	MAT	MH
Heating efficiency of BCR on SLST	0,56	0,63	0,59	0,41	-0,42	-0,47
Heating efficiency of BCR on WLST	0,36	0,37	0,21	0,29	-0,21	-0,01
Cooling efficiency of BH on SLST	-0,47	-0,56	-0,13	0,18	0,07	-0,24
Cooling efficiency of BH on WLST	-0,43	-0,52	-0,33	-0,11	0,31	0,45
Cooling efficiency of SDR on SLST	-0,62	-0,72	-0,31	0,06	0,23	0,17
Cooling efficiency of SDR on WLST	-0,45	-0,56	-0,32	-0,06	0,31	0,46
Cooling efficiency of TH on SLST	0,02	0,04	0,39	0,02	-0,31	-0,31
Cooling efficiency of TH on WLST	-0,26	-0,39	-0,69	-0,45	0,72	0,45

5. Discussions and conclusions

This study proposed a new framework for quantifying the specific temperature changes caused by various morphological features, by integrating cities, scales, and seasons. The applied partial dependence plot (PDP) can not only quantify the positive or negative association between independent morphological features and LST, but also provide a useful tool to extract the maximum heating or cooling effect of each feature. These results indicated that the PDP can effectively replace the Pearson correlation analysis and fill the gap that traditional relative importance cannot bridge in linking urban morphology to temperature and making comparisons among different cities.

5.1 Influencing mechanisms of dominant morphological features on LST

Building coverage ratio, building height, surface developed ratio, and tree height were found to contribute the most to the variations of LST at different scales, which is consistent with previous research (Li et al., 2021; Li and Hu, 2022). The specific heating or cooling efficiency of each feature differs, which can be explained based on the theory of urban energy balance. When horizontal heat advection is not considered, the energy absorbed from solar radiation and the anthropogenic heat are balanced through heating the surrounding air temperature and through heat storage and evapotranspiration (Oke, 1988).

- The building coverage ratio is positively related to LST. A densely built landscape can reduce surface reflections, leading to an increase in net solar radiation and corresponding sensible heat flux, which continuously heats the surrounding environment (Chun and Guldmann, 2014). Additionally, a high building coverage allows for less open space, which may weaken urban ventilation, cause heat accumulation, and further increase the heating effect.
- Building height and surface fluctuations are negatively related to LST. High buildings generate more building shades, which helps to shield downward shortwave radiation and create a local cooling effect. In China, high buildings are usually surrounded by wider roads (Guo et al., 2021). Although these roads are covered by asphalt and cement with high specific heat capacity, their heat storage is relatively less during satellite observation time (around 11:00 am in China), and the wider roads create a better ventilation path for heat removal.
- The cooling effect of trees was found to be much stronger than that of building height and fluctuation. The effects of tree height on LST may be twofold. Firstly, denser nearby vegetation provides cooling by blocking direct solar radiation, and higher trees with dense foliage can create more shade. Secondly, the higher albedo of vegetation leads to more

reflected solar radiation. Additionally, evapotranspiration contributes significantly to cooling the surrounding area, particularly during the summer.

5.2 Seasonal variations of the heating or cooling effect of dominant morphological features

The heating or cooling efficiency differs across cities and seasons. For building coverage ratio, the heating effect during summer is much higher than that during winter because the solar radiation is stronger during summer. This leads to an increase in net solar radiation, generating more sensible heat flux based on energy balance, which together create a warmer environment than the same morphology condition during winter. Similar seasonal differences are also observed by tree height, but the differences in the northern cities are much more significant than those in the south. In the northern cities, the dominant vegetation type is deciduous broad-leafed forest (Fig. 7), therefore the latent heat flux and shade are weaker due to less solar radiation, bare trees, and frozen water during winter, resulting in a lower cooling effect. In the southern cities with warm winters, the larger leaves of evergreen broad-leafed forest and tropical rainforests result in less decrease in the albedo and shade of the southern vegetation than that of the northern part, maintaining a relatively stable cooling effect.

Figure 7. Spatial distribution of vegetation types in China mainland.

The cooling efficiency of building height and surface fluctuation during winter was stronger than that during summer, which is opposite to the trend for building coverage ratio and tree height. During summer, the stronger solar radiation generates more sensible heat flux, which warms the surroundings even under building shade, resulting in weaker cooling efficiency. During winter, weaker solar radiation results in less sensible heat flux to warm the surroundings, and more urban heat is carried away due to cold winds. Additionally, the lower solar elevation angle leads to larger

and longer building shade area, further enhancing the cooling effect. These factors together lead to a stronger cooling efficiency, particularly around high-rise buildings in the north.

5.3 Potential factors affecting heating or cooling and suggestions for urban planning

Higher economic levels and greater population concentrations lead to an increase in the heating efficiency of building coverage ratio, and a decrease in the cooling efficiency of building height and surface fluctuation. Concentrated economic activities and urban populations are associated with more energy consumption, traffic congestion, and greenhouse gas emissions, which can lead to an increase in anthropogenic heat (Stewart and Oke, 2012). Against the backdrop of global warming, cities are increasingly vulnerable to extreme weather events such as flooding and heatwaves (WMO, 2022), and the impact of urban morphology on seasonal LST is closely linked to economic development. In this context, there is an urgent need for efficient and feasible policies for local adaptation to environmental risks, particularly those related to heat management (IPCC, 2022). Given that the compound effects of solar radiation and anthropogenic heat on LST differ between cities and seasons, we propose the following recommendations:

- **Measures to increase the albedo.** Increasing urban green vegetation with large leaf cover and high height could potentially be applied to urban temperature mitigation, particularly during summer in the north. For commercial and industrial areas, new materials with green roofs could be considered to reflect incoming solar radiation and accelerate heat dissipation. Traditional residential regions could also consider adding more vegetation cover to buildings and walls, which could not only alter local urban temperature but also make communities more environmentally friendly and livable. Moreover, the vernacular architecture and roads are composed of materials with green bricks, grey tiles, and wood, which can both retain traditional architecture characteristics and yield lower temperature due to higher albedo.

- **Optimization of urban building layouts.** The community is the basic unit of activity for urban dwellers in China, with large communities consisting of up to hundreds of buildings and small communities consisting of just a few buildings. The spatial layout of buildings is important for both old and new communities. Dense buildings not only contribute to higher LST during the summer but also affect the amount of sunlight during the winter. For old communities, planned demolition may be necessary to create more regular and open building patterns. The resulting open space and diverse patterns can be used for more green space, improving the local urban heat environment and water cycle through evapotranspiration.
- **Optimization of urban ventilation paths** should be considered, considering the wind-blocking effect of high-density buildings. The overall design of the block should reserve ventilation gaps to maximize the introduction of external airflow into the interior of the block. An open building layout also helps to create as much ventilation space as possible, which can be useful for mitigating temperature during summer. In order to avoid excessive heat dissipation during winter, one possible solution is that the buildings in northern cities could be designed perpendicular to the direction of prevailing winds, avoiding the formation of strong wind zones.

5.4 Limitations and further application

The conclusions of this study still require further experimentation, because, firstly, the selected cities in this study are mostly located along the east shore, where the latitude significantly influences climate features. To obtain a more precise conclusion, more influencing factors and cities should be chosen, considering the estimated land area of 9.6 million km^2. Secondly, this study only considered the seasonal influence and failed to consider the diurnal influence of urban morphology on the urban heat environment. As the intensity of incoming solar radiation varies

throughout the day, the impacts of urban morphology on the urban thermal environment change within a 24-hour cycle (Wang et al., 2023). However, most of the satellites for retrieving LST are polar-orbiting satellites that have a fixed earth observation time. The ECOsystem Spaceborne Thermal Radiometer Experiment on Space Station (ECOSTRESS), which provides atmospherically corrected LST products with a spatial resolution of 70 m and a recycling period of 3-5 days, can help address this issue (Fisher et al., 2020). In contrast to polar satellites, the International Space Station can generate LST products at different times of the day with an overall accuracy of 1K (Fisher et al., 2020). In the future, our focus will be on studying how the influence of urban morphology on LST changes within the diurnal cycle across cities and scales.

The framework proposed in this study may provide one possible solution for further evaluation of the regional and global influence of urbanization on climate change. In fast-developing countries such as China, India, and Brazil, urbanization has a significant impact on urban morphology, but quantifying the specific influence on urban temperature remains challenging for researchers. The key issue is how to generate accurate 3D building models, including building footprints and height information. Bing Maps has detected over 900 million buildings around the world and released the dataset online (https://github.com/microsoft/GlobalMLBuildingFootprints). The development of high-resolution remote sensing technology has provided reliable data sources on built forms, which offer a variety of products on building heights to the public at national, continental, and global scales (Frantz et al., 2021; Esch et al., 2022; Wu et al., 2023). Together with our methods, these data sources allow for large-scale comparisons of temperature changes among regions, and are conducive to seeking efficient urban adaptation strategies for long-term environmental changes.

Appendix

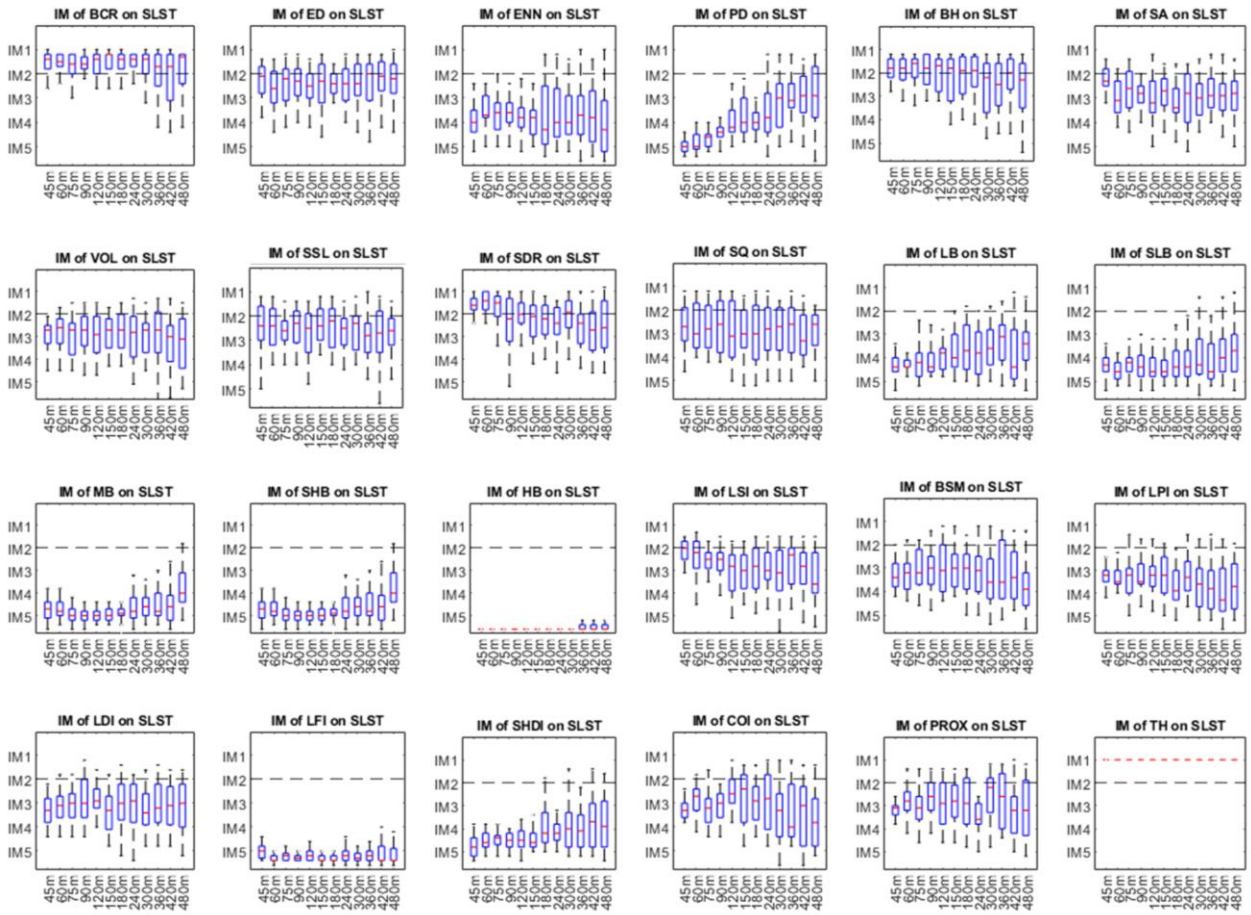

Figure A1. Changes of relative importance for each morphological feature among scales during summer. Each box means the relative importance set for all cities at a specific scale, and the red line in the box represents the median value. The dotted line is the dividing line between IM1 and IM2.

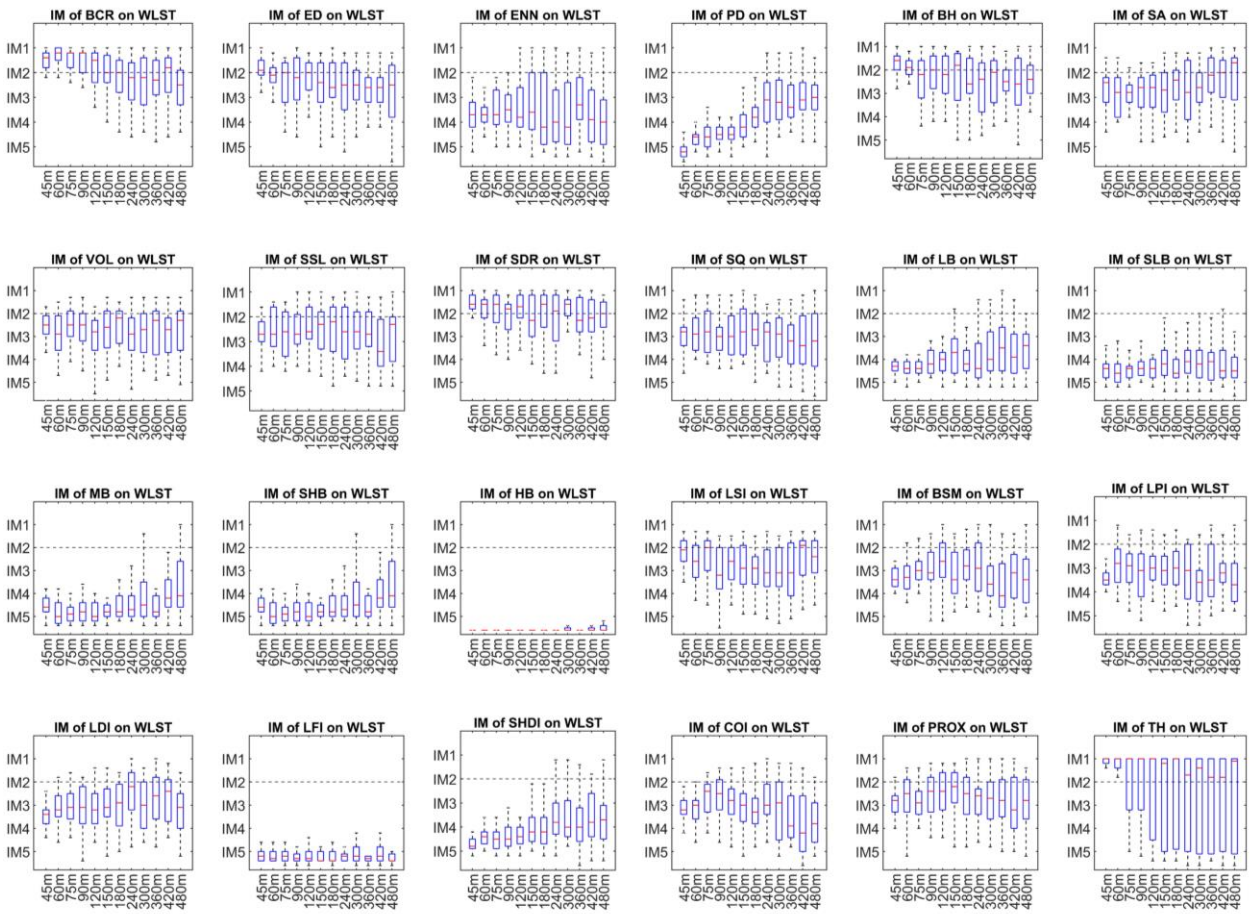

Figure A2. Changes of relative importance for each morphological feature among scales during winter. Each box means the relative importance set for all cities at a specific scale, and the red line in the box represents the median value. The dotted line is the dividing line between IM1 and IM2.

References

Baccini M, Biggeri A, Accetta G, et al. Heat effects on mortality in 15 European cities[J]. *Epidemiology*, 2008: 711-719.

Beck H E, Zimmermann N E, McVicar T R, et al. Present and future Köppen-Geiger climate classification maps at 1-km resolution[J]. *Scientific data*, 2018, 5(1): 1-12.

Belgiu M, Drăguţ L. Random forest in remote sensing: A review of applications and future directions[J]. *ISPRS journal of photogrammetry and remote sensing*, 2016, 114: 24-31.

Berger C, Rosentreter J, Voltersen M, et al. Spatio-temporal analysis of the relationship between 2D/3D urban site characteristics and land surface temperature[J]. *Remote sensing of environment*, 2017, 193: 225-243.

Chun B, Guldmann J M. Spatial statistical analysis and simulation of the urban heat island in high-density central cities[J]. *Landscape and urban planning*, 2014, 125: 76-88.

Esch T, Brzoska E, Dech S, et al. World Settlement Footprint 3D-A first three-dimensional survey of the global building stock[J]. *Remote Sensing of Environment*, 2022, 270: 112877.

Ewing R, Rong F. The impact of urban form on US residential energy use[J]. *Housing policy debate*, 2008, 19(1): 1-30.

Fisher J B, Lee B, Purdy A J, et al. ECOSTRESS: NASA's next generation mission to measure evapotranspiration from the international space station[J]. *Water Resources Research*, 2020, 56(4): e2019WR026058.

Frantz D, Schug F, Okujeni A, et al. National-scale mapping of building height using Sentinel-1 and Sentinel-2 time series[J]. *Remote Sensing of Environment*, 2021, 252: 112128.

Gao X, Wang X, Zhu B. The distribution of Chinese minority populations and its change based on the study of the Hu Huanyong line[J]. *International Journal of Anthropology and Ethnology*, 2017, 1: 1-16.

Gao Y, Zhao J, Han L. Quantifying the nonlinear relationship between block morphology and the surrounding thermal environment using random forest method[J]. *Sustainable Cities and Society*, 2023: 104443.

Gauthier, P.; Gilliland, J. Mapping urban morphology: a classification scheme for interpreting contributions to the study of urban form. *Urban Morphol* 2006, 10, 41–50.

Gorelick N, Hancher M, Dixon M, et al. Google Earth Engine: Planetary-scale geospatial analysis for everyone[J]. *Remote sensing of Environment*, 2017, 202: 18-27.

Guo F, Hu D, Schlink U. A new nonlinear method for downscaling land surface temperature by integrating guided and Gaussian filtering[J]. *Remote Sensing of Environment*, 2022, 271: 112915.

Guo F, Schlink U, Wu W, et al. Differences in Urban Morphology between 77 Cities in China and Europe[J]. *Remote Sensing*, 2022, 14(21): 5462.

Guo F, Wu Q, Schlink U. 3D building configuration as the driver of diurnal and nocturnal land surface temperatures: Application in Beijing's old city[J]. *Building and Environment*, 2021, 206: 108354.

Han H, Guo X, Yu H. Variable selection using mean decrease accuracy and mean decrease gini based on random forest[C]//2016 7th ieee international conference on software engineering and service science (icsess). IEEE, 2016: 219-224.

He B J, Zhao D, Xiong K, et al. A framework for addressing urban heat challenges and associated adaptive behavior by the public and the issue of willingness to pay for heat resilient infrastructure in Chongqing, China[J]. *Sustainable cities and society*, 2021, 75: 103361.

Hu D, Meng Q, Schlink U, et al. How do urban morphological blocks shape spatial patterns of land surface temperature over different seasons? A multifactorial driving analysis of Beijing, China[J]. *International Journal of Applied Earth Observation and Geoinformation*, 2022, 106: 102648.

Huang X, Wang Y. Investigating the effects of 3D urban morphology on the surface urban heat island effect in urban functional zones by using high-resolution remote sensing data: A case study of Wuhan, Central China[J]. *ISPRS Journal of Photogrammetry and Remote Sensing*, 2019, 152: 119-131.

Hutengs C, Vohland M. Downscaling land surface temperatures at regional scales with random forest regression[J]. *Remote Sensing of Environment*, 2016, 178: 127-141.

IPCC, 2022: Climate Change 2022: Impacts, Adaptation, and Vulnerability. Contribution of Working Group II to the Sixth Assessment Report of the Intergovernmental Panel on Climate Change [H.-O. Pörtner, D.C. Roberts, M. Tignor, E.S. Poloczanska, K. Mintenbeck, A. Alegría, M. Craig, S. Langsdorf, S. Löschke, V. Möller, A. Okem, B. Rama (eds.)]. Cambridge University Press. Cambridge University Press, Cambridge, UK and New York, NY, USA, 3056 pp.

Kedron P, Zhao Y, Frazier A E. Three dimensional (3D) spatial metrics for objects[J]. *Landscape Ecology*, 2019, 34: 2123-2132.

Li H, Li Y, Wang T, et al. Quantifying 3D building form effects on urban land surface temperature and modeling seasonal correlation patterns[J]. *Building and Environment*, 2021, 204: 108132.

Li Z, Hu D. Exploring the relationship between the 2D/3D architectural morphology and urban land surface temperature based on a boosted regression tree: A case study of Beijing, China[J]. *Sustainable Cities and Society*, 2022, 78: 103392.

Liu H, Huang B, Zhan Q, et al. The influence of urban form on surface urban heat island and its planning implications: Evidence from 1288 urban clusters in China[J]. *Sustainable Cities and Society*, 2021, 71: 102987.

Logan T M, Zaitchik B, Guikema S, et al. Night and day: The influence and relative importance of urban characteristics on remotely sensed land surface temperature[J]. *Remote Sensing of Environment*, 2020, 247: 111861.

Lu H, Li F, Yang G, et al. Multi-scale impacts of 2D/3D urban building pattern in intra-annual thermal environment of Hangzhou, China[J]. *International Journal of Applied Earth Observation and Geoinformation*, 2021, 104: 102558.

Moudon A V. Urban morphology as an emerging interdisciplinary field[J]. *Urban morphology*, 1997, 1(1): 3-10.

Oke T R. The urban energy balance[J]. *Progress in Physical geography*, 1988, 12(4): 471-508.

Oke T R, Mills G, Christen A, et al. *Urban climates*[M]. Cambridge University Press, 2017.

Peng J, Xie P, Liu Y, et al. Urban thermal environment dynamics and associated landscape pattern factors: A case study in the Beijing metropolitan region[J]. *Remote Sensing of Environment*, 2016, 173: 145-155.

Sexton J O, Song X P, Feng M, et al. Global, 30-m resolution continuous fields of tree cover: Landsat-based rescaling of MODIS vegetation continuous fields with lidar-based estimates of error[J]. *International Journal of Digital Earth*, 2013, 6(5): 427-448.

Song J, Chen W, Zhang J, et al. Effects of building density on land surface temperature in China: Spatial patterns and determinants[J]. *Landscape and Urban Planning*, 2020, 198: 103794.

Stewart I D, Oke T R. Local climate zones for urban temperature studies[J]. *Bulletin of the American Meteorological Society*, 2012, 93(12): 1879-1900.

Wang Q, Wang X, Meng Y, et al. Exploring the Impact of Urban Features on the Spatial Variation of Land Surface Temperature within the Diurnal Cycle[J]. *Sustainable Cities and Society*, 2023: 104432.

World Meteorological Organization (WMO). (2022). State of the Global Climate 2021 (Issue WMO-No. 1290). WMO. https://library.wmo.int

Wu Q, Li Z, Yang C, et al. On the scale effect of relationship identification between land surface temperature and 3D landscape pattern: The application of random forest[J]. *Remote Sensing*, 2022, 14(2): 279.

Wu Q, Tan J, Guo F, et al. Multi-scale relationship between land surface temperature and landscape pattern based on wavelet coherence: the case of metropolitan Beijing, China[J]. *Remote Sensing*, 2019, 11(24): 3021.

Wu W B, Ma J, Banzhaf E, et al. A first Chinese building height estimate at 10 m resolution (CNBH-10 m) using multi-source earth observations and machine learning[J]. *Remote Sensing of Environment*, 2023, 291: 113578.

Wu W B, Yu Z W, Ma J, et al. Quantifying the influence of 2D and 3D urban morphology on the thermal environment across climatic zones[J]. *Landscape and Urban Planning*, 2022, 226: 104499.

Yang J, Wang Y, Xiao X, et al. Spatial differentiation of urban wind and thermal environment in different grid sizes[J]. *Urban Climate*, 2019, 28: 100458.

Ye X, Rogerson P. The impacts of the modifiable areal unit problem (MAUP) on omission error[J]. *Geographical Analysis*, 2022, 54(1): 32-57.

Yu S, Chen Z, Yu B, et al. Exploring the relationship between 2D/3D landscape pattern and land surface temperature based on explainable eXtreme Gradient Boosting tree: A case study of Shanghai, China[J]. *Science of the Total Environment*, 2020, 725: 138229.

Zhao L, Lee X, Smith R B, et al. Strong contributions of local background climate to urban heat islands[J]. *Nature*, 2014, 511(7508): 216-219.

Declaration of Competing Interest

The authors declare that they have no known competing financial interests or personal relationships that could have appeared to influence the work reported in this paper.